Study State of Thermal Analysis of Multi Effect Desalination (MED) by Using Equal Temperature Deference Scheme

[1]Bashir A. Aburwin, [1]Faraj E. El-sager and [3]Amhmed M. Alaela

[1]Faculty of Engineering, Tripoli University, Tripoli, Libya
[2]Higher Institute of Technical Agriculture Algeran Tripoli, Libya

Abstract: Mathematical modeling of the multi effect distillation (MED) process has been carried out to determine the effects of the important design and operating variables on the parameters controlling the cost of producing fresh water. The model of MED assumes equal temperature difference through each evaporator and also the same procedure through each feedwater preheater at all effects. In addition, the model considered the impact of the vapor leak in the venting system, the variation in thermodynamic losses from one effect to another, the dependence of the physical properties of water on salinity and temperature and the influence of noncondensable gases on the heat transfer coefficients in the evaporators and the feed preheaters. Results show that the plant Gain Output Ratio (GOR) is weakly related to the top brine temperature at low number of effects and strongly related to the number of effects. The specific heat transfer area increases by raising the number of effects and reducing the top brine temperature. The effect of the top brine temperature on the specific heat transfer area is more pronounced with a larger number of effects. The specific flow rate of cooling seawater increases with the increasing of the top brine temperature and by the decrease in number of effects.

Key words: Gain output ratio GOR % Specific heat transfer area sA % Specific flow rate of cooling seawater sMcw

INTRODUCTION

The MED processes are based on using heat to vaporize a portion of the treated fluid. The various evaporation processes represent differences in energy conservation and reuse. Saline solutions are made to boil again and again, without the addition of any heat, by successively reducing the pressure. A process diagram for the forward-feed Multiple Effect Distillation (MED) sea water desalination process is shown in the Fig. 1. The effects are numbered 1 to n from the left to right (the direction of the heat flow). The feed and vapor flow concurrently in the direction of the falling pressure. The system consists of a number of evaporators, n, a series of feed water preheaters, a train of flashing boxes, last effect or bottom condenser and a venting system. The MED has n effect. On the other hand, the upper number of effects is imposed by the difference between the heating steam temperature T_S and the boiling point in the last effect T_n. The MED has n-2 feed preheater, while the MED has n-1 of flashing boxes. Each effect constitutes of a heat transfer area, vapor space mist eliminator and other accessories [1].

The horizontal falling film evaporator is the most widely used in the MED desalination process. The major advantage of the horizontal falling film evaporator is its ability to handle sea water scaling, due to high wetting rates and efficient water distribution over the heat transfer surfaces by large spray nozzles.

A controlled amount of sea water $(\dot{m}_{CW} + \dot{m}_f)$ is introduced into the down condenser associated with the last effect, where its temperature increases from the sea water temperature t_{CW} to t_f. Part of this water $\dot{m}_{CW}$ is rejected back to the sea. The function of circulation water $\dot{m}_{CW}$ in the last stage condenser is the removal of the excess heat added to the system in the first effect. It is worth mentioning that the evaporators do not consume most of the supplied heat, it simply downgrades it.

Corresponding Author: Bashir A. Aburwin, Faculty of Engineering, Tripoli University, Tripoli, Libya.
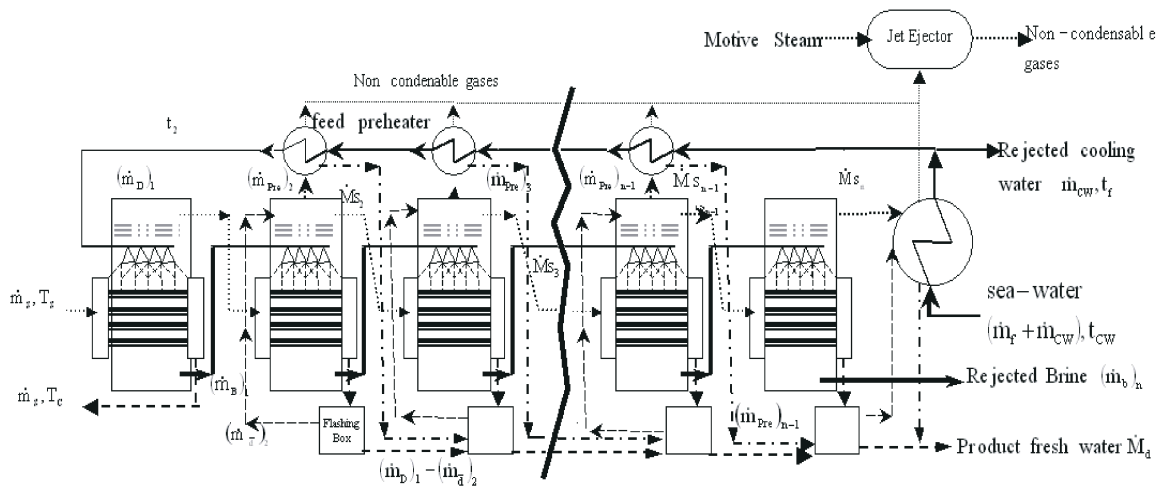
Fig. 1: Process flow diagrams for the multiple effect distillation (MED) desalination process

The remaining part of sea water $\dot{m}_f$ at t_f is chemically treated, deaerated and pumped through the preheaters. Feed preheating is an important means of improving the system performance ratio or Gain output ratio (GOR). The temperature of the feed water increases from t_f to t_2 as it flows inside the tubes of the preheaters. The heat necessary to heat the feed water is supplied by condensing a portion of vapor $(\dot{m}_{pre})_i$ formed in each effect (i) at the shell side of the preheaters. The feed water $\dot{m}_f$ is sprayed at the top of the first effect, where it falls as a form of thin film down the succeeding rows of tubes arranged horizontally. Within this effect, the brine temperature raises to the boiling temperature corresponding to the pressure in the vapor space T_1 before a small portion of vapor $(\dot{m}_D)_1$ is evaporated. The heat required to preheat the feed and for evaporating $(\dot{m}_D)_1$ is released by condensing a controlled mass of saturated steam $\dot{m}_S$ inside the tube bundle.

The temperature of the vapor formed in the first effect Tv_1 is less than the boiling temperature T_1 by the boiling point elevation (BPE$_1$). The vapor generated therein flows through a knitted wire mist separator known as a wire mesh demister to remove the entrained brine droplets. The saturation temperature of the vapor departing the demister is less than that of the formed vapor temperature due to the frictional pressure loss in the demister. The vapor flows from the demister have to be transported to the second effect. This transport inevitably involves a pressure drop and hence a corresponding decreases in the saturation temperature. Another pressure fall and consequent depression in the saturation temperature of the vapor is associated with vapor condensation inside

the heat transfer tubes in the evaporators or over the heat transfer area in the preheaters. The latent heat of condensation of $(\dot{m}_D)_1$ exploited for further evaporation in the second effect. The remaining un evaporated brine in the first effect ($\dot{m}_f - (\dot{m}_D)_1$) or $(\dot{m}_B)_1$ goes to the second effect, which operates at a lower pressure.

The vapor is formed inside the second effect by two different mechanisms. First, by boiling over heat transfer surfaces $(\dot{m}_D)_2$. Second, by flashing or free boiling within the liquid bulk $(\dot{m}_d)_2$. The temperature of the vapor formed by flashing Tv_2 is less than the effect boiling temperature T_2 by the boiling point elevation (BPE)2 and the non equilibrium allowance (NEA)$_2$. Another small quantity of vapor $(\dot{m}_{\bar{d}})_2$ is formed in the flashing box due to the flashing of distillate condensed in the second effect $(\dot{m}_D)_1$. The flashed off vapor $(\dot{m}_{\bar{d}})_2$ is produced at a temperature Tv_2 which is lower than the condensation temperature of distillate Tc_1 by the non equilibrium allowance (NEA)$_2$. The flashing boxes offer a way to recover heat from condensed fresh water. The boiling point elevation (BPE) and temperature depression corresponding to pressure loss in the demister $)T_m$, transmission lines $)T_t$ and during the condensation process $)T_C$ reduces the available driving force for heat transfer in the evaporators and the preheaters [1]. The portion of mass vapor $(\dot{m}_{pre})_2$ formed by each evaporating, flashing the effect and the flashing box is condensed on the shell side of the preheater. In this paper the $\dot{m}_{pre}$ is not equal to $\dot{m}_{\bar{d}}$ which was considered in [1]. The heat given up results in a heating of the brine flowing inside the preheater tubes. The distillate condensed in the preheater $(\dot{m}_{pre})_2$ is carried with the condensed water
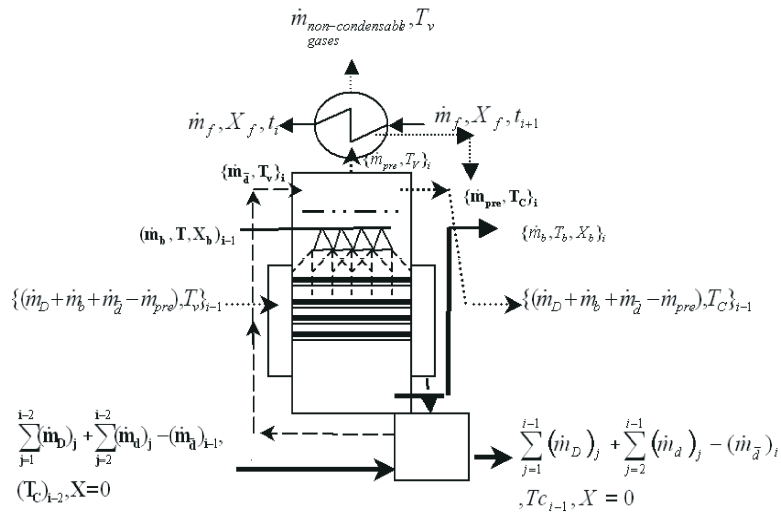
Fig. 2: The entries and the exits of variables and parameters in typical effect (i).

formed by condensing $\left[\dot{m}_D + \dot{m}_d + \dot{m}_{\bar{d}} - \dot{m}_{pre}\right]_2$ or $(\dot{M}_S)_2$ into the tubes of the third effect. Although the vapors formed by evaporation and flashing are drawn separately in the flow diagram to show the process, they flowed from the evaporator and the flashing box to the feed heater in the same line. The processes that take place in the second effect are repeated in each effect all the way down to the last. The Fig. 2. shows the entries and the exits of variables and parameters in typical effect (i). It is worth mentioning that the amount of steam generated by evaporation in each effect is less than the amount generated in the previous effect. This is due to the increase in the specific latent heat of vaporization with the decrease in the effect temperature. Consequently, the amount of vapor generated in an evaporator by boiling is less than the amount of condensing steam used for heating in the following evaporator. The non evaporated brine flowing into the last effect reaches its final concentration X_n by evaporating more vapors. The remaining brine $\dot{m}_b$ is rejected to the sea. The vapor formed by boiling and flashing in the last effect $(\dot{m}_D + \dot{m}_d)_n$ and in the end flashing box $[\dot{m}_{\bar{d}}]_n$ passes to the bottom condenser. The condenser and the brine heaters must be provided with good vents, first for purging during start-up and than for remove noncondensable gases, which may have been introduced with the feed or drawn in through leaks to the system.

The presence of the noncondensable gases not only impedes the heat transfer process but also reduces the temperature at which steam condenses at the given pressure. This occurs partially because of the reduced partial pressure of vapor in a film of poorly conduction gas at the interface. The help conserver steam economy venting is usually cascaded from the steam chest of one preheater to another. The effects operate above atmospheric pressure are usually vented to the atmosphere. The noncondensable gases are always saturated with vapor. The vent for the last condenser must be connected to vacuum-producing equipment to compress the noncondensable gases to the atmosphere. This usually a steam jet ejector if high-pressure steam is available. Steam jet ejector is relatively inexpensive but also quite inefficient [1].

Since the vacuum is maintained on the last effect, the no evaporated brine flows by itself from effect to effect and only a blow down pump is required in the last effect.

MATERIALS AND METHODS

The analysis of MED system is based on developing a steady state mass and energy balances coupled with the heat transfer rate correlations for each individual effect and conjoining them with the ratio between the mass of feed to that of product fresh water. The generated vapor has a saturation temperature T_v corresponding to the pressure in the evaporator vapor space. This temperature is less than the boiling temperature T_i by the boiling point elevation (BPE), also the generated vapor depends upon thermal resistance of heat transfer area A_e.

$$T_i = (T_v)_i + BPE_i +) T_h \qquad (1)$$

The boiling point rise caused by the hydrostatic head) Th has a negligible effect in the horizontal falling film evaporators. The BPE at a given pressure is the increase in the boiling temperature due to the salts dissolved in the water. The boiling point elevation BPE_i is calculated from the following empirical formula [2].

$$BPE_i = \times_i (B + C*\times_i)* 10^6 \tag{2}$$

where:

$$B = (6.71 + 6.34 \times 10^{-2} T_i + 9.74 \times 10^{-5} T_i^2)* 10^{-3} \tag{3}$$
$$C = (22.238 + 9.59 \times 10^{-3} T_i + 9.42 \times 10^{-5} T_i^2)*10^{-8} \tag{4}$$

The above equation is valid over the following ranges: $20000 < X < 160000$ ppm, $20 < T < 180°C$. The dimension of the evaporator heat transfer area of first effect A_{el} is function of the thermal resistance and the temperature driving force obtained from the amount of heat transfer Q_1 the overall heat transfer coefficient of evaporator U_o and the temperature difference of condensing steam T_s and the boiling brine. The heat transfer area on the first effect is represented by:

$$A_{e_1} = \frac{Q_1}{U_o (T_S - T_1)} \tag{5}$$

where Q_1 is the heat transfer rate for the first effect. The effects of steam superheating and condensate subcooling have negligible roles on the heat transfer process in the evaporator of the MED system.

The overall heat transfer coefficient based on the outside surface area U_o is calculated by using the following expression.

$$\frac{1}{U_o} = \frac{r_o}{h_{e\,in}\ r_{in}} + R_{f\,in}\ \frac{r_o}{r_{in}} + \frac{r_o\ \ln(r_o/r_{in})}{k_w} + R_{f\,o} + \frac{1}{h_{e\,o}} \tag{6}$$

where h is the heat transfer coefficient, $R_{f\,in}$ and $R_{f\,o}$ are the fouling resistance of inside and outside of tube respectively, k_w is the thermal conductivity of tube material, r_{in} and r_o are radiuses of inside and outside of tube surfaces respectively.

The evaporator heat transfer surface area A_{el} is usually, but not always taken as that contact with the boiling liquid, whether on the inside or the outside of the tubes. Han and Fletcher [3] developed the following experimental correlation to calculate the boiling heat transfer coefficient h_{eo} for thin water film flowing over the outside of smooth horizontal tubes.

$$h_{eo}\left[\frac{\mu^2}{r^2\ g\ k^3}\right]^{\frac{1}{3}} = 0.0004\ Re^{0.2}\ Pr^{0.65}\ q''^{0.4} \tag{7}$$

In the above equation Re and Pr are Reynolds and Prandle numbers, respectively, q‼ is the heat flux, μ is the viscosity, D is the density and k is the thermal conductivity of the fluid. The above correlation is valid over the following ranges:

$770 \# Re \# 7000$, $1.3 \# Pr \# 3.6$, $30 \# q'' \# 80$ kW $/ m^2$ and $49 \# T \# 127°C$.

The maximum deviation for the equation is ± 10 %.

The heat transfer coefficient of condensation inside a horizontal tube for a particular flow pattern h_{in}. However, the correlations, which can be used for all flow patterns are limited. Perhaps the most verified predictive general technique available for all flow regimes in horizontal tubes is the following correlation of Shah [4]:

$$\frac{h_{in}}{h_f} = 1 + \frac{3.80}{const^{0.95}} \tag{8}$$

The parameter Z is defined as :

$$const = \left[\frac{1}{\overline{X}} - 1\right]^{0.8} Pr^{0.4} \tag{9}$$

where: O is the vapor mass fraction, The local superficial heat transfer coefficient h_f calculated from:

$$h_f = h_\ell (1 - \overline{x})^{0.8} \tag{10}$$

where h_f is the heat transfer coefficient, when all the flowing mass is liquid and is calculated by the well-known Dittus-Bolter equation,

$$h_\ell = 0.023\ (Re)^{0.8}\ (Pr)^{0.4}\left[\frac{k}{d_{in}}\right] \tag{11}$$

The above correlation is valid over the following ranges:

$2.8\# *_{in} \# 40$ mm, $21 \# T_v \# 355° C$, $0 \# O \# 1$, $0.158 \# q'' \# 16000$ kw $/m^2$, $11 \# G_1 \# 4000$ kg/m² s, $0.7 \# P \# 1$ bar, $0.0019 \# Pr \# 0.82$, $350 \# Re \# 100000$.

The average heat transfer coefficient h_{ein} is obtained by liner interpolation between the values of local heat transfer coefficient h_{in} at the values of the vapor mass fraction O ranging from 0.01 to 0.99.

Proper venting of the evaporator reduces significantly the impairing effects of the noncondensable gases on the condensation heat transfer coefficient. Continuous withdrawal of gases prevents their accumulation and minimizes their effect on the heat transfer coefficient. A decrease of less than 5 % occurs in the heat transfer coefficient for a gas concentration of the 10 % in the vent stream. Standiford modeled the effect of noncondensable gases in water desalination plants; the volumetric concentration of noncondensable gases is about 4 % [5].

Boiling and flashing mechanisms form the vapor in the second effect or other effects accept 1st effect. Boiling takes place over the outer surface of the heating surface.

$$(\dot{m}_D)_1 = (\dot{M}s_1 I_1)/I_2$$

In general

$$(\dot{m}_D)_i = (\dot{M}s_{i-1} I_{i-1})/I_i \qquad (12)$$

The amount of vapor flashed off from the brine flowing to the next effect or other effects $\dot{m}_d$ is estimated from equation.

$$(\dot{m}_d)_i = \frac{(\dot{m}_b)_i \ \bar{C}p_i \ (T_{i-1} - T_i')}{l_i} \qquad (13)$$

The temperature $T!_i$ is higher than the boiling temperature by the non equilibrium allowance $(NEA)_i!$. That is.

$$T_i' = T_i + (NEA)_i' \qquad (14)$$

The is a measure for the efficiency of the flashing process. Miyatake, *et al*. [6] developed the following equation to correlate data obtained from flash evaporation experiments in a pool of pure water, which simulates to the flashing process inside the evaporators and the flashing boxes.

$$(NEA)_i' = \frac{33.0 \ \Delta T_i^{0.55}}{(T_v)_i} \qquad (15)$$

where
$)T_i = T_{i-1} - T_i,$
$(T_v)_i = T_i - (BPE)_i \qquad (16)$

The pressure loss in the demister is during the vapor flow through demister, which is widely used as the mist eliminator in water desalination industry, which the dry

steam passed wire mesh pad free of any entrained droplets, the pressure loss through the mesh pad is given by.

$$\Delta P_m = \frac{ff \ W_m \ a \ r_V \ V_v^2}{g \ e^3} \qquad (17)$$

where V_v is the vapor superficial velocity (m / s), a is the specific area per unit volume (approximately $= 85 - 115 \ m^2 / m^3$), D_v is the vapor density, g is the bed void fraction (varied from 0.97 to 0.99) W_m is the mesh pad thickness and ff is the friction factor. The value of ff depends mainly on the extent of the modified Reynolds number as follows:

$$ff = 7.5 \ Re^{-0.6} \quad 10 < Re < 100 \qquad (18)$$
$$= 3.37 \ Re^{-0.43} \quad Re > 100$$

The pressure drop $)p_t$ in the lines connecting the vapor space in effect (i) and the evaporator tubes of next effect (i+1), can be calculated from the Unwind formula [1].

$$\Delta P_t \frac{0.0001306 \ \dot{M}_S^2 \left(1.0 + \dfrac{3.6}{d_i}\right) L_t}{r_V \ d_i^5} \qquad (19)$$

where L_t is the length of the connecting lines, $*_i$ is the pipe inside diameter, $\dot{M}_S$ is the vapor mass flow rate inner pipe.

The pressure drop during the vapor condensation inside the evaporator tubes $)P_C$ is the sum of the frictional $)P_r$ gravitational $)P_g$ and deceleration $)P_a$ components. That is:

$$)P_C =)P_r - ()P_g +)P_a) \qquad (20)$$

The two terms on the right hand side of Eq. (20) have opposite signs. The first gives a fall in pressure due to wall friction. While the second represents a rise in pressure because of the pressure recovery from the flow deceleration and the gravitational force. For the condensation inside horizontal tubes, the gravitational component of the pressure drop ÄPg is equal to zero. However, it is usual to design the condenser with a small angle of inclination such that the condensate tends to run out of the end of the tubes at the opposite end to the steam inlet. This makes the flow much more stable than if the tubes are horizontal. It also improves the efficiency of the venting system. This component of pressure drop is estimated from this expression:

$$)p_g = (D_V " + (1-")D_R)gZsinM \qquad (21)$$

where " is the vapor phase void fraction, Z is the pipe length and M is the inclination angle. There are many correlations for the void fraction ". The one suggested most frequently in the literature for condensation in tube is by Zivi [7].

$$a = \frac{1}{\left[1 + \frac{1-\bar{X}}{\bar{X}}\left[\frac{r_n}{r_\ell}\right]^{0.5}\right]} \quad (22)$$

The acceleration pressure drop is calculated from this formula.

$$Term = \frac{\bar{x}^2}{a\,r_v} + \frac{(1-\bar{X})^2}{(1-a)\,r_\ell}$$

$$)p_a = G^2(Term_{in} - Term_{out}) \quad (23)$$

The two-phase pressure losses due to the friction (dP_r / dZ) are generally expressed as a function of the corresponding single-phase pressure losses, which is multiplied by a correction factor 2_R^2 that is given by:

$$q\,_\ell^2 = \frac{(dP_r/dZ)}{(dP_r/dZ)_\ell} \quad (24)$$

The fractional pressure gradient calculated from the Fanning equation [8].

$$\left[\frac{dP_r}{dZ}\right]_\ell = \frac{2.0\,f_{fo}\,G_\ell^2}{r_\ell\,d_{in}} \quad (25)$$

The friction factor expressed in terms of the Reynolds number by the Blasius equation [8].

$$f_{fo} = 0.079\,Re_\ell^{\left(-\frac{1}{4}\right)} \quad (26)$$

Friedel [9] developed the following correlation for calculating 2_1^2.

$$Per = \left[\frac{r_\ell}{r_n}\right]^{0.91}\left[\frac{V_v}{V_\ell}\right]^{0.19}\left[1 - \frac{V_v}{V_\ell}\right]^{0.7}$$

$$XFrac = 3.24\,\bar{X}^{0.78}(1.0 - \bar{X})^{0.24}$$

$$q\,_\ell^2 = E + \frac{Per \times XFrac}{Fr^{0.045}\,We^{0.035}}$$

where,

$$E = (1-\bar{X})^2 + \bar{X}^2\left[\frac{r_\ell\,f_v}{r_v\,f_\ell}\right] \quad (28)$$

$$Fr = \frac{G^2}{g\,d_{in}\,r_{TP}^2} \quad (29)$$

$$We = \frac{G^2\,d}{s\,r_{TP}} \quad (30)$$

where f_v and f_L are the friction factors for the total mass flux flowing with vapor and liquids, respectively. G is the mass flux, μ is the dynamic viscosity and F is the surface tension.

$$f_L = \frac{64}{Re_L} \quad (31)$$

And

$$f_v = \frac{64}{Re_V} \quad (32)$$

The density of the two phase mixture D_{TP} is defined as:

$$r_{TP} = \left[\frac{\bar{X}}{r_n} + \frac{(1-\bar{X})}{r_\ell}\right]^{-1} \quad (33)$$

Hewitt [10] recommended the use of Friedel equation when the value of (μ_1 / μ_v) is less than 1000. In the MED system this ratio ranges from 65.12 at T= 315 K to 19.856 at T= 385 K. The frictional pressure drop term usually calculated in a stepwise manner. The tube is divided into a number of short lengths $)Z$ over which the conditions change only moderately. The temperature depression or the vapor saturation temperature decrease $(T_v–T_c =)T_v)$, due to the pressure drop in the demister $)P_m$, vapor transmission line $)P_t$ and during condensation process $)P_c$, the pressure drop into the Demister, Transmission lines, Condensation $)P_{mtc}$ are:

$$)p_{mtc} = ()P_m +)P_t +)P_c) \quad (34)$$

After rearrangement,

$$P_c = P_v -)P_{mtc} \quad (35)$$

The temperature T_C of saturated liquid at P_C, it predicted from the steam tables.

The mass of vapor $(\dot{m}_{\bar{d}})_i$ formed by flashing in each flashing box is given by the following:

$$(\dot{m}_{\bar{d}})_i = \left[\sum_{j=1}^{i-1}(\dot{m}_D)_j + \sum_{j=2}^{i-2}(\dot{m}_d)_j\right]\bar{C}_p(T_{Ci-1} - T_i'')/l_i \quad (36)$$

where: $\overline{c}_p$ is the average specific heat over the temperature range of interest and:

$$T_i{!!} = (T_v)_i + NEA_i{!!} \tag{37}$$

$NEA_i{!!}$ is the non equilibrium allowance inside flashing box i:

$$NEA_i'' = \frac{0.33\,(Tc_{i-1} - Tv_i)}{Tv_i} \tag{38}$$

The condensation temperature Tc_{i-1} of vapor inside the tube bundle of the next effect, Tc_{i-1} is less than the boiling point temperature in the previous effect T_{i-1} by the boiling point elevation $(BPE)_{i-1}$ and the saturation temperature depression associated with the pressure loss during the vapor flow in the demister $()\,T_m)_{i-1}$, vapor transmission lines $()\,T_t)_{i-1}$ and vapor condensation inside the horizontal tubes $()\,T_C)_{i-1}$. Thus,

$$(T_c)_{i-1} = T_{i-1} - (BPE +)\,T_m +)\,T_t +)\,T_C)_{i-1} \tag{39}$$

The heat balance around the feed preheater is:

$$\dot{m}_f \cdot Cp(t_i - t_{i+1}) = h_p(\dot{m}_{pre} - \dot{m}_{non-condensable})_i \cdot 1_i' \tag{40}$$
$$\text{gases}$$

The efficiency 0_{pi} accounts for the heat loss to the surrounding and the vapor escape with the vented noncondensable gases.

The condensation temperature T'_c for each preheater is calculated from the following equations:

$$T'_c = T' -)\,T_m -)\,T_C \tag{41}$$

where $)\,T_m$ and $)\,T_C$ are the temperature losses corresponding to the pressure drop associated with the vapor flow through the demister pad and vapor condensation outside the tubes of the preheater. Eq. (41) predicts the pressure drop due to the vapor flow through the demister. On the other hand, the pressure drop due to the vapor flow over the preheater tubes can be calculated, at best, only roughly because changing velocity and flow pattern during condensation process. This overall pressure drop associated with the vapor condensation process is the algebraic sum of the pressure losses due to the vapor flow in the nozzles and headers static pressure head, two phase friction loss and momentum the condensers. The momentum change or flow slow down during condensation results in a pressure recovery. The magnitude of this pressure recovery is high in vacuum operation. The pressure regain can approach or exceed the friction loss. Since most effects in MED plants operator at vacuum, it seems reasonable to assume that the pressure recovery due the flow slow down can compensate for the friction pressure drop component; therefore, the net pressure fall and consequently the saturation temperature depression in the condensation process can be neglected. The heat transfer between the condensing vapor and the sea water in the feed preheater of the second effect can be written in terms of an overall heat transfer coefficient Up, preheater heat transfer area Ap and the logarithmic mean temperature difference LMTD, thus:

$$\dot{m}_f\ Cp\,(t_i - t_{i+1}) = h_i\,(\dot{m}_{pre} - \dot{m}_{non-condensable})\,1_i'$$
$$\text{gases} \tag{42a}$$
$$= Up_i\ Ap_i\ (LMTD)_i$$

The $(LMTD)_i$ is expressed as:

$$(LMTD)_i = \frac{t_i - t_{i+1}}{1n\,\dfrac{(T'_{Vc})_i - t_{i+1}}{(T'_{Vc})_i - t_i}} \tag{42}$$

Combining Eqs. (40.a) and (42) produces:

$$\frac{(T'_{Vc})_i - t_{i+1}}{(T'_{Vc})_i - t_i} = Exp\left[\frac{U_p\ A_P}{\dot{m}_f\ C_p}\right]_i = Exp(NTU_P)_i \tag{43}$$

where $(NTU_P)_i$ is the number of transfer units. Eq(43) was solved for the outlet temperature of feed water to give:

$$t_i = T'_{Cv} (T'_{Cv} t_{i+1})\,Exp(-NTU_P)_i \tag{44}$$

The term $(T!_{Cvi} - t_i)$ is the preheater terminal temperature difference and its value has a strong impact on the preheater heat transfer area, t_i is the feed water temperature left preheater(i).

Eqs. (5, 6) can be used to relate the overall heat transfer coefficient of preheater(i) Up_i to the individual coefficients.

The inside tube heat-transfer coefficient of preheater h_i is calculated from the empirical formula developed by Dittus & Boelter which can be found in any heat transfer handbook.

$$h_i = \overline{A}\left(\frac{K_b}{D_i}\right)\,Re^{\overline{B}}\ Pr^{\overline{C}} \tag{45}$$

where $\overline{A}$, $\overline{B}$, $\overline{C}$ are constants as 0.023, 0.8, 0.4 respectively.

In the other hand, Khan *et al.* [11], developed the following equation to calculated the heat transfer coefficient during vapor condensation outside the tubes.

$$(\mathbf{h_o})_i = \left[\mathbf{0.725} \left(\frac{\mathbf{k} \ell^3 \ \mathbf{r_\ell} \ (\mathbf{r_\ell} - \mathbf{r_n}) \ \mathbf{g} \ \mathbf{l_i}}{(\mathbf{d_o} \ \mathbf{m} \Delta \mathrm{T})^{0.25}} \right) \mathbf{C_1} \ \mathbf{C_2} \right]_i \quad (46)$$

The correction factors C_1 and C_2 consider the influence of the condensate dripping down and the presence of noncondensable gases, when they constitute less than 4 % by weight. On the condensation heat transfer coefficient, respectively. The size of the coefficients C_1 and C_2 are given by the following equations:

$C_1 = 1.23795 + 0.353808 N - 0.0017035 \ N^2$ (47)
$C_2 = 1 - 34.313 \ X_{nc} + 1226.8 \ X^2_{nc} - 14923 \ X^3_{nc}$ (48)

where X_{nc} is the percentage weight of the noncondensable gases and N is the number of tube rows in the vertical direction inside the condenser. The value of N depends on the total number of tubes N_t tube arrangement pitch Pt, number of tube passes and nozzle diameter. It is customary practice to arrange the tubes in the feed heaters with a square pitch pattern to provide adequate mechanical cleaning for the outer surface of the tubes. In these arrangements each four tubes occupy an area of $(4 \ Pt^2)$ and the number of tubes in the vertical direction are two tubes. Thus, the total number of tubes, which can be installed in a shell of diameter Ds and with a pitch of Pt, can be approximated by this equation:

$$N_t = \frac{\mathbf{p} \ Ds^2}{4 \ Pt} \quad (49)$$

The following relation determines the number of tubes in the vertical direction N to the shell diameter and pitch:

$$\mathbf{N} = \frac{\mathbf{Ds}}{\sqrt{\mathbf{2Pt}}} = \mathbf{0.564} \sqrt{\mathbf{N_t}} \quad (50)$$

For tubes arranged in an equilateral triangular pitch. The following equation can be used:

$N = 0.481 \ (N_t)^{0.505}$ (51)

The total number of tubes in the feed heater is calculated by:

$$\mathbf{N_t} = \frac{\dot{\mathbf{M}}_\mathbf{f} \ \bar{\mathbf{C}}_\mathbf{p} \ (\mathbf{t_i} - \mathbf{t_{i+1}})}{(\mathbf{U_P})_\mathbf{i} \ \mathbf{p} \ \mathbf{d_o} \ \mathbf{Z_p} \ (\mathbf{LMTD})_{\mathbf{p \ at \ i}}} \quad (52)$$

$$= \frac{\mathbf{4.0} \ \dot{\mathbf{M}}_\mathbf{f}}{\mathbf{p} \ \mathbf{d^2_{in}} \ \mathbf{r_\ell} V_p}$$

where Z_p is the tube length of preheater, $*_o$ and $*_{in}$ are the tube outside and inside diameters respectively and V_p is the feed water velocity. The value of V_p is limited at the top end by erosion damage to the tube materials and excessive pumping costs and at the bottom end by higher fouling rates and the need to maintain high side heat transfer coefficients. It ranges in thermal desalination units, between 1.3 – 2.2 m/s.

There are two basic distinctions between the feed preheaters of any effect and the last effect condenser. The first one is the mass of vapor condensed in the shell side, the vapor formed by boiling and flashing inside the last evaporator and flashing box $(\dot{m}_D + \dot{m}_d + \dot{m}_{\bar{d}})_n$. The other difference is that the mass of water flowing inside the tubes of the last condenser and the feed water plus the cooling water $(\dot{m}_{CW} + \dot{m}_f)$. Accordingly, the following relationships can be developed for the last effect condenser.

$$h_{condencer}(\dot{m}_D + \dot{m}_d + \dot{m}_{\bar{d}})_n \cdot l'_n =$$
$$(\dot{m}_f + \dot{m}_{cw}) \cdot Cp_f(t_f - t_{cw}) = \left(U \ A(LMTD) \right)_{condenser} \quad (53)$$

$$t_f = T'_n - e^{-(NTU)} \ (T'_n - T_{cw}) \quad (54)$$

where: T_{cw} is the sea water temperature and $\dot{m}_{cw}$ is the mass flow rate of cooling water. Arranging the above two equations and substituting the value of (LMTD) condenser from Eqn. (53) produces:

$$\dot{m}_{cw} = \frac{h_{condencer}(\dot{m}_D + \dot{m}_d + \dot{m}_{\bar{d}} - \dot{m}_{non-condensable})_n \cdot l'_n}{Cp_f(t_n - t_{cw})} - \dot{m}_f \quad (55)$$

The water production cost focuses on reduction of the capital investment and the operating cost of the different desalination processes. The capital investment of the thermal desalination units depends on the number of separation effects, the specific heat transfer area and the type of construction material. the other hand, the specific energy consumption, the maintenance requirements affect the operating cost. The selection of the optimum top brine temperature of the MED process

depends on the specific heat transfer area, the thermal performance ratio and specific cooling seawater. The first of these parameters affects the capital investment of the process and the second two parameters control the operating cost. Thus, the important design and operating variables on the parameters controlling the cost of producing fresh water are the Gain Output Ratio, the specific heat transfer area and the specific flow ratio of cooling water. The Gain output ratio GOR of the forward MED plant is defined as the mass of distillate water produced per unit mass of heating steam used. That is:

$$GOR = \frac{\dot{M}_d}{\dot{m}_s} \tag{56}$$

where: $\dot{M}_d$ is the total mass of distillate formed by boiling and flashing in all effects and flashing box, $\dot{m}_S$ is the mass of heating steam of forced heating in the 1st effect. Thus:

$$\dot{M}_d = \sum_{1}^{n}(\dot{m}_D)_i + \sum_{2}^{n}(\dot{m}_d + \dot{m}_{\bar{d}})_i \tag{57}$$

The specific heat transfer surface area, sA defined as the total heat transfer area of the plant per mass of distillate water produced.

$$sA = \frac{\sum_{i=1}^{n} Ae_i + \sum_{i=2}^{n-1} Ap_i + Ac}{\dot{M}_d} \tag{58}$$

where: Ae_i is the heat transfer surface area of effect(i), Ap_i is the heat transfer surface area of preheater(i), Ac is the total heat transfer surface area of down condenser. The specific cooling water flow rate, sMcw defined as mass of cooling water per mass of distillate water produced.

$$sMcw = \frac{\dot{m}_{CW}}{\dot{M}_d} \tag{59}$$

where $\dot{m}_{cw}$ is the mass of rejected cooling seawater [kg/s].

Solution of the Problem: The steady state equations of the developed model with the empirical correlations are solved to simulate the MED desalination process.

Therefore, an iterative solution is necessary to calculate the system variables and parameters. The mathematical model of MED system is solved iteratively effect by effect using the well-known Gauss-Seidel iteration scheme. The parameters controlling the cost of producing fresh water calculations are the plant gain output ratio GOR, the specific heat transfer surface area sA and the specific flow rate of cooling water sMcw.

Those parameters are computed as a function of the most important design variables, called top brine temperature TBT and the number of effects n. The system with equal temperature difference distribution scheme was analyzed firstly, i.e., between top brine temperature and rejected brine temperature of the last effects uniformly distribute temperature difference, the temperature difference between preheaters are the same temperature difference between feed water temperature at down condenser to feed water temperature at 1st evaporator. The flow rate of vapor generated outside the tube and condensate inside the tube and area of evaporator and salinity concentration and also the mass product vapor for both brine flashing and flashing box for each effect were obtained by solving the equations numerically (iteratively).

RESULTES AND DESCUSIONS

The results of the MED desalination plant model have been presented in terms of the following thermal characteristics parameters:

C   The Gain Output Ratio, GOR; is measured by the kg of distillate water produced per kg of heating steam condensed in the first effect.

C   The Specific Heat Transfer Surface Area; sA defined as the total heat transfer area of the plant per mass of distillate water produced.

C   The Specific Cooling Water Flow Rate; sMcw defined as mass of cooling water per mass of distillate water produced.

The Gain Output Ratio, GOR: The impacts of the top brine temperature and the number of effects on the gain output ratio has been analyzed. Its found that this ratio is weakly dependent on the top brine temperature especially at low number of effects (n) and is strongly dependent on the number of effects (n), The gain output ratio has lower value at higher top brine temperatures (TBT). The gain output ratio GOR improved by 2.0 times from TBT at 112°C, when n is 5 effects to TBT is 62°C, when n equals 11 effects. The obtained results are presented in Fig. 3. Moreover, the impacts can be explained by the following reasons:

C   An increase in the amount of sensible heating required to increase the feed seawater temperature to the boiling temperature.

C   A decrease in the latent heat of the heating steam at higher temperatures.
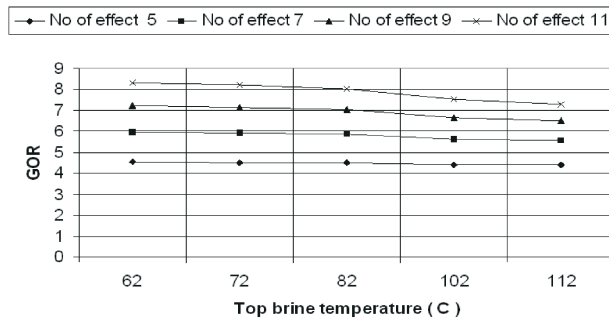
Fig. 3: The variation of the plant gain output ratio with both the top brine temperature and the number of effects.
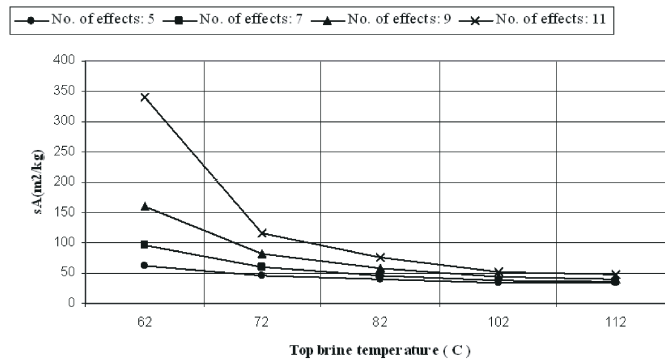

Fig. 4: Influence of top brine temperature and number of effects on the specific heat transfer area
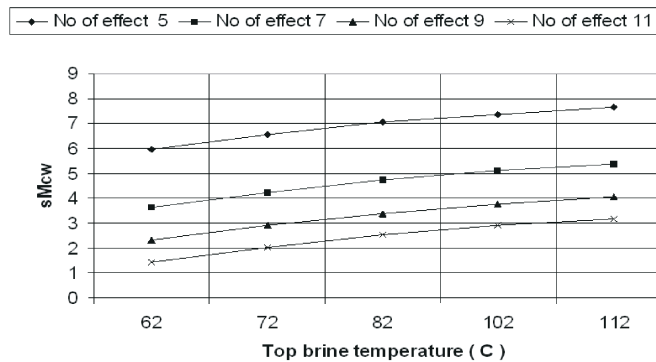

Fig. 5: Effect of top brine temperature and number of effects on the specific flow rate of the cooling water

In other words, the number of effects is directly linked to the number of reusing the heating steam in generating nearly the same amount of this steam.

The Specific Heat Transfer Surface Area, sA: Figure 4 depicts the influence of the top brine temperature and the number of effects on the specific heat transfer area. The specific heat transfer area decreases rapidly as the top brine temperature increases, where the sA decreased by 25 times from TBT is 62°C to TBT is 112°C at n equals 11 effects, but the sA decreased by 1.8 times from TBT is 62°C to TBT is 112°C at n equals 5 effects. It can also be observed that, the specific heat transfer area increases as the number of effects are increased, where the sA decreased by 23.5 times from n equals 11 effects to n equals 5 effects at TBT is 62°C, but the sA decreased only 1.25 times at TBT is 112°C from n equals 11 effects to n equals 5 effects. The reasons can be illustrated as following:

C   The increase in heat transfer coefficient as a result of change in the values of the physical properties of the brine and condensing vapor, especially the liquid phase viscosity, which enhances the rate of heat transfer in either stream.

C The increase in the temperature driving force per effect, which increases the deriving force for heat transfer. For the same number of effects, this behavior is obtained as a result of increasing the top brine temperature and keeping the last effect temperature constant at 40°C.

The Specific Cooling Water Flow Rate, sMcw: The question of the influence of the top brine temperature and number of distillation effects on the specific flow rate of the cooling water is addressed and given in Fig. 5.

It is clearly observed that, the specific flow rate of cooling seawater increases with the increase of the top brine temperature, where the sMcw decreased by 2.12 times from TBT is 62°C to TBT is 112°C at n equals 11 effects, but the sMcw decreased by 1.28 times from TBT is 62°C to TBT is 112°C at n equals 5 effects. This is caused by the decrease in the system Gain Output Ratio at the top brine temperatures, which implies an increase in the specific thermal energy of the system. At higher top brine temperatures the temperature drop per effect increases and results in an increase in the amount of vapor formed per effect. This increases the amount of vapor formed in the last effect and therefore increase in the amount of cooling seawater.

CONCLUSIONS

The Thermal analysis of the MED desalination plant model leads to the following important conclusions:

C The GOR for MED plant is higher at law top brine temperatures and larger number of effects, for illustration the GOR improved by 2.0 times from TBT is 112°C and n equals 5 effects to TBT is 62°C and n equals 11 effects.

C The specific heat transfer area for MED plant decreases drastically at higher operating temperatures, due to the fact that the sA decreased by 25 times from TBT is 62°C to TBT is 112°C, when n equals 11 effects, Hence the specific heat transfer area increases as the number of effects are increased, because of the sA decreased by 23.5 times from n equals 11 effect to n equals 5 effects at TBT is 62°C.

C The specific cooling water increases by increase of top brine temperature and increases by decrease number of effects, where the sMcw decreased by 2.188 times from TBT is 62°C to TBT is 112°C when n equals 11 effects, but the sMcw decreased by 1.28 times from TBT is 62°C to TBT is 112°C at n equals 5 effects.

Table 1: The major differences between the present study and the study of [1]

|	Present study	Dessouki and Ettouney study
1	All interned mass vapor to next evaporator or preheater was variable, such as $(\dot{M}_S)_i$, $(\dot{m}_{pre})_i$ where $(\dot{M}_S)_i$ is apportion of mass vapor generated within effect(i) $(\dot{m}_{pre})_i$ is complement mass vapor generated within effect(i)	Fixed interned mass vapor to next evaporator or preheater. Where $(\dot{M}_S)_i = (\dot{m}_D)_i$ $(\dot{m}_{pre})_i = (\dot{m}_d)_2 + (\dot{m}_{\overline{d}})_2$
2	Solution of modeling by using equal temperature difference distribution scheme	Solution of modeling by using equal heat transfer area scheme
3	Rejected brine salinity was 70 g/l, it can be changed.	Not mentioned
4	Unknown variables for each effect A_e, A_{pre}, Xb, $\dot{m}_D$, $\dot{m}_B$, $\dot{m}_d$, $\dot{m}_{\overline{d}}$, X_n	Unknown variables for each effect T, X_b, $\dot{m}_D$, $\dot{m}_B$, $\dot{m}_d$, $\dot{m}_{\overline{d}}$
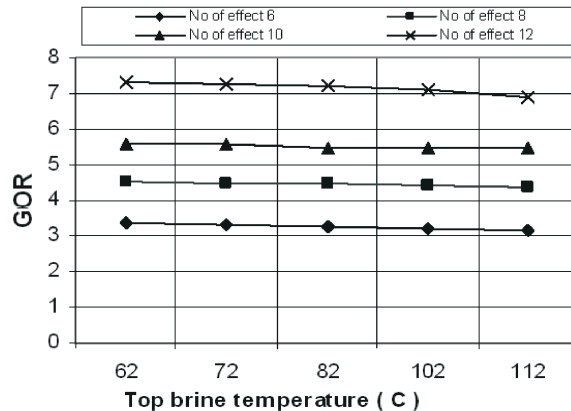
Fig. 6: The variation of the plant gain output ratio with both the top brine temperature and the number of effects for EL-Dessouki, H. T and Ettouney paper
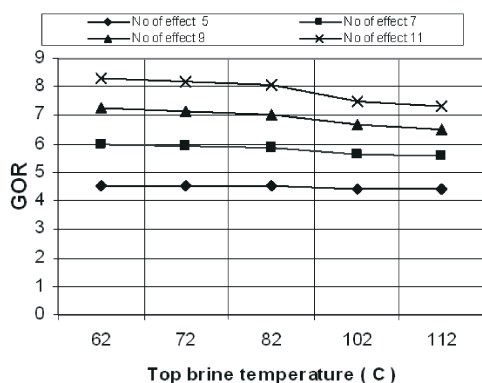
Fig. 3: The variation of the plant gain output ratio with both the top brine temperature and the number of effects for present paper

C   The obtained results of the present paper have been further compared with the results which were obtained from EL-Dessouki, H. T and Ettouney [1]. The main differences between the present study and the study given by EL-Dessouki, H. T and Ettouney hes been summarized in Table 1.

Some comparative analysis between the results of present paper and EL-Dessouki, H. T and Ettouney paper have been addressed in terms of the computed GOR variable of top brine temperature and number of effects.

The variation of the plant gain output ratio with both the top brine temperature and the number of effects for the present study was showed in Figure 3. while Figure 6. showed the variation of the plant gain output ratio with both the top brine temperature and the number of effects for the EL-Dessouki, H. T and Ettouney. It observed that GOR for the present study was higher than that of [1]. This discrepancy in results between the two models due to some improvements introduced in the present paper those depicted in Table 1.

REFERENCES

1. EL-Dessouki, H.T. and H.M. Ettouney, 1998. Steady-State Analysis of the Multiple Effect Evaporaton Desalination Process, chem. Eng. Techncl., 21(5).
2. EL-Dessouki, H.T. and H.M. Ettouney, 1999. Single effect thermal vapor compresion Desalination process: Thermal Analysis, 20(2).
3. Han, J. and L. Fletcher, 1985. Ind. Eng. Chem. Process Desa. Dev., 24: 570-597.
4. Shah, M.M., 1978. Heat Transfer, Pressure Drop, Visual Observations, Test Data for Ammonia Evaporating Inside Tubes, ASHRAE Trars., 84 Part 2.
5. Standiford, F.C., 1984. Evaporators and Evaporation, Encyclopedia of chemical Processing and Design (Meketta, Ed.) Vol. 20, Marcel Dekker, Inc., NY.
6. Miyatake, O., K. Murakami and Y. Kawata, 1973. Fujii, Heat Transfer Jpn. Res., 2: 89-100.
7 Zivi, S.M., 1964. J. Heat Transfer, 86: 247-252.
8. Collier, J.G., 1980. Convective Boiling and Condensation, J. Wily.
9. Friedel, L., 1977. New Friction Pressure Drop Correlations for Upward. Horizontal and Downward Two-Phase Pipe Flow, proceedings of the HTFS Symposium, Oxford.
10. Hewitt, G.F., 1982. Gas-Liquid, in: Handbook of Multiphase systems, Hemisphere Publishing. NY.
11 Khan, 1986. Desalination and Purification 1, Elsevier, Amsterdam.

Nomeclature:

Cp Specific heat at constant pressure over the temperature T

$\overline{C}_p$ Average specific heat over the temperature range of interest.

$£_{in}$ Heat transfer coefficient inside tube

$£_O$ Heat transfer coefficient outside tube

$£_f$ Local superficial heat transfer coefficient

$£_R$ Heat transfer at liquid flow.

Lt length of the connecting lines between evaporators of MED

t The temperature of feedwater flowing inside the preheaters.

Tc Condensed vapor temperature

w_m Demister thickness of MED

8 Latent heat associated to temperature T

8! Latent heat associated to temperature T!

Rf_{in} The thermal resistance of the fouling at inside diameter

Rf_o The thermal resistance of the fouling at outside diameter

U_o The heat transfer coefficient over tube bundle in evaporator of MED

O_p Thermal efficiency of preheaters of MED

g Gravitational acceleration m/sec2.

G_R Mass flux of liquid, [kg/ (m² sec)]

μ Dynamic viscosity (kg/m.sec)

D Density of flow (kg/m³)

X The salt concentration, ppm

F Surface tension, N/m

L Specific volume of flow, m³/kg

TDS Total dissolved salts, ppm